Dispersion of gas flaring emissions in the Niger delta

Fawole, Olusegun; Cai, Xiaoming; Abiye, Olawale; Mackenzie, Angus

DOI:
10.1016/j.envpol.2018.12.021

Accepted Manuscript

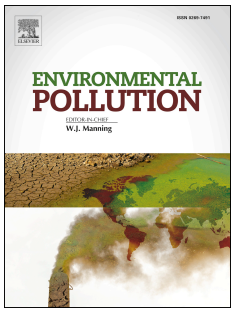

Dispersion of gas flaring emissions in the Niger delta: Impact of prevailing meteorological conditions and flare characteristics

Olusegun G. Fawole, Xiaoming Cai, Olawale E. Abiye, A.R. MacKenzie

PII: S0269-7491(18)33983-6

DOI: https://doi.org/10.1016/j.envpol.2018.12.021

Reference: ENPO 11961

To appear in: *Environmental Pollution*

Received Date: 1 September 2018

Revised Date: 29 November 2018

Accepted Date: 8 December 2018

Please cite this article as: Fawole, O.G., Cai, X., Abiye, O.E., MacKenzie, A.R., Dispersion of gas flaring emissions in the Niger delta: Impact of prevailing meteorological conditions and flare characteristics, *Environmental Pollution* (2019), doi: https://doi.org/10.1016/j.envpol.2018.12.021.

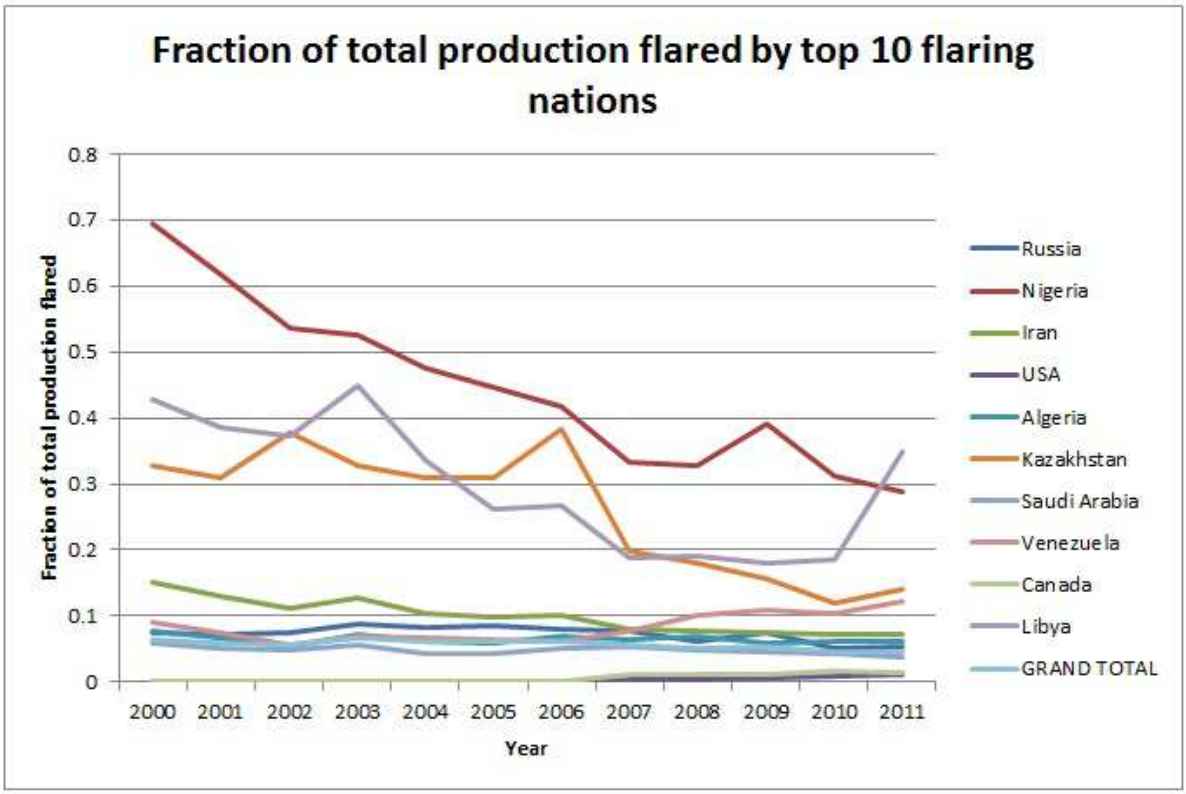

Dispersion of gas flaring emissions in the Niger Delta: Impact of prevailing meteorological conditions and flare characteristics.

Olusegun G. Fawole* [1, 2], Xiaoming Cai [2], Olawale E. Abiye [4], A.R. MacKenzie [2, 3]

[1] Department of Physics and Engineering Physics, Obafemi Awolowo University, Ile-Ife, Nigeria 220005

[2] School of Geography, Earth and Environmental Sciences, University of Birmingham, B15 2TT, UK

[3] Birmingham Institute of Forest Research (BIFoR), University of Birmingham, B15 2TT, UK

[4] Centre for Energy Research and Development (CERD), Obafemi Awolowo University, Ile-Ife, Nigeria 220005

[*] Corresponding author: gofawole@oauife.edu.ng

Abstract

An understanding of the dispersion and level of emissions source of atmospheric pollutants; whether point, area or volume sources, is required to inform policies on air pollution and day-to-day predictions of pollution level. Very few studies have carried out simulations of the dispersion pattern and ground-level concentration of pollutants emitted from real-world gas flares. The limited availability of official data on gas flares from the oil and gas industries makes accurate dispersion calculations difficult. Using ADMS 5 and AERMOD, this study assessed the sensitivity of dispersion and ground-level concentration of pollutants from gas flares in the Niger Delta to prevailing meteorological condition; fuel composition; and flare size. Although, during the non-WAM (West African Monsoon) months (November and March), the simulated ground-level concentrations of pollutants from a single flare are lower, the dispersion of pollutants is towards both the inland and coastal communities. In the WAM months, the ground-level concentrations are higher and are dispersed predominantly over the inland communities. Less buoyant plumes from smaller flares (lower volume flow rates) and/or flaring of fuel with lower heat content results in higher ground-level concentrations in areas closer to the flare. Considering the huge number of flares scattered around the region, a mitigation of the acute local pollution level would be to combine short stacks flaring at lower volume flow rates to enhance the volume flow rate of a single exhaust, and hence, the buoyancy of the plume exiting the stack.

Main finding

Flare and fuel characteristics significantly affects the dispersion pattern and ground-level concentration of pollutants. There is greater population dose during the non-WAM months.

1 Introduction

Poor air quality is a persistent problem in major cities and industrialised regions of the world. This problem poses significant threat to the environment, plants and humans. Gaseous and particulate air contaminants have been strongly linked with health problems in human and animals (Gryparis et al., 2004; Kampa and Castanas, 2008; Pope III, 2000; Pope III et al., 2002; Pope III and Dockery, 2006), poor yield in plants (Adole, 2011; Dung et al., 2008) and climate forcing (IPCC, 2013). These pollutants are emitted by different sources which could be classified as either *natural* or *anthropogenic*. The nature and size of the sources vary significantly, and hence, the nature and quantity of the pollutants they emit. As a result of the varying nature of the sources, air pollutants are released into the ambient air at different rates and varying conditions.

With an estimated daily production of 2.7 million barrels, Nigeria is currently ranked 12th on the list of crude oil producing nations of the world (OPEC, 2015). In Nigeria, the exploration and exploitation of crude oil has contributed, in no small measure, to degradation of the environment of the oil producing communities and worsening air quality of the West Africa sub-region (Ana et al., 2012; Anomohanran, 2012; Dung et al., 2008; Fawole et al., 2017). The Niger Delta, the oil producing region of Nigeria, contains over 300 active flare sites scattered around residential communities and farm lands (Elvidge et al., 2015), where over a quarter of the annual total natural gas production is flared (Fawole et al., 2016a; Ite and Ibok, 2013). In 2008, it was estimated that about 15.1 billion cubic meter (bcm) of natural gas was flared in the region (Elvidge et al., 2009). Remoteness of exploration sites, non-availability of market, and inadequate piping to transport the gas, are some of the reasons for the continuous and persistent gas flaring in the region. Gas flaring is a prominent source of carbon monoxide

(CO), carbon dioxide (CO_2), NO_X ($NO+NO_2$), soot (predominantly black carbon (BC)) and poly aromatic hydrocarbon (PAH), especially in oil-producing regions of the world (Ana et al., 2012; Johnson et al., 2013; USEPA, 2011; USEPA, 2012).

The geometry of flares - height, inclination and diameter - differs from one flow station to another. These geometry plays a prominent role in the dispersion of emissions from flares (Turner, 1994; Zannetti, 2013). Emissions from high temperature combustion processes, such as power generation, industrial facilities, and gas flares have much higher release temperatures compared to the ambient air. On their release from their stacks, these high temperatures make them highly buoyant. The combined effect of both the buoyancy and momentum of emissions from the stack causes the plume to rise above the initial height of the stack and enhances near-source dispersion (Arya, 1999). Due to their unique nature and feature; such as, buoyancy of hot plume, dispersion of emissions from this class of emission sources differs from passive sources (MoE Ontario, 2009).

The composition of natural gas varies significantly from one flow station to another. These varying compositions play prominent roles in the combustion parameters of the gas (Fawole et al., 2016a). Combustion parameters such as heat content, net heat released, buoyancy flux and momentum flux are major determinants of the plume rise and, hence, the dispersion pattern and trend of emissions from gas flares.

Prevailing meteorology is of utmost importance in the dispersion of emission from any emission source. Wind speed, wind direction and atmospheric stability play greater roles in the meandering and dispersion of emission in the plume releases, whether buoyant or non-buoyant (Arya, 1999; Zannetti, 2013). The West Africa region, and hence, the Niger Delta, witnesses strong reversal of wind directions as a result of the movement of the intertropical convergence zone (ITCZ) and intertropical front (ITF) (Sultan and Janicot, 2000; Sultan and Janicot, 2003) resulting in the West African Monsoon (WAM). The WAM months (April –

September) are characterised by heavy rainfall and prevailing south-westerly winds while the non-WAM months (November – March) are often extremely dry months characterised by Harmattan (cold and very dry dusty winds) and prevailing North-easterly winds (Marais et al., 2014).

Atmospheric Dispersion Modelling System (ADMS) is a robust state-of-the-science Gaussian dispersion model developed by the Cambridge Environmental Research Consultant (CERC) and is on the list of alternative dispersion models recommended by the United State Environmental Protection Agency (USEPA). The American Meteorological Society/Environmental Protection Agency Regulatory Model (AERMOD) is an advanced Gaussian-based regulatory air pollution dispersion model. ADMS and AERMOD are arguably the most widely used near field dispersion models within the environmental science community. Both have been used to simulate the dispersion of pollutants emitted from a range of source types and validated across a range of atmospheric and terrain conditions (Abiye et al., 2016; Carruthers et al., 1997; Connan et al., 2011; Heist et al., 2013). ADMS and AERMOD use Monin–Obukhov similarity to define the structure of the planetary boundary layer and then computes the steady-state Gaussian solutions to describe the dispersion of pollutants (Heist et al., 2013). For details of the runs and meteorological set-up of the window-based version of AERMOD used in this study see Abiye et al., (2016).

In this study, using ADMS 5 and window-based version of AERMOD, we investigate the impact of prevailing meteorology during the peak periods of the WAM and non-WAM months, flare size and fuel compositions on the dispersion of emissions from gas flares in the Niger Delta area of Nigeria. In addition to establishing typical dispersion characteristics for gas flaring in Nigeria, the study discusses possible mitigation options for the most acute local pollution.

Section 2 gives a detailed description of the study site and prevailing meteorological condition at the site. Section 3 presents an in-depth description of the combustion parameter, emission factors applied and other experimental variables while section 4 gives a breakdown of the results from ADMS and AERMOD simulations including an extensive discussion of the results and their implications.

2 Study Area

The Niger Delta, situated in the southern part of Nigeria, is bordered by the Gulf of Guinea on the South and located between 4.3 – 7.7^{o} N and 4.4 – 9.5^{o} E. All the oil exploration facilities in Nigeria are located in the Niger Delta. More than 900 active oil wells (Osuji and Onojake, 2004) and over 300 active flares are scattered around the region. According to 2009 estimates, the region's 75,000 km^2 landmass is occupied by about 31 million people (Young, 2013). Figure 1 show the Niger Delta and the locations of active flares scattered around the region. Of the 325 active flare sites identified in the Nigeria oil field in 2012, 97 (~ 30 %) rank among the top 1000 largest flares of the 7467 individual flares identified globally (Fawole et al., 2016b). From the inception of oil exploration over four decades ago, gas flaring activities in the study area has been a persistent daily activity in the several flow stations and rigs.

The quality of ambient air in the study site is arguably at its lowest ebb. Last year, there were incidents of several soot episodes that lasted for days in Port-Harcourt, a major city in the region. Although, there are other sources of air pollution in the region, petroleum industries scattered around the region has been identified as the major source of air pollutants (Ede and Edokpa, 2015). The quality of ambient air in the Niger Delta is bad and quite worrisome. Adoki (2012) found that pollutants in ambient air around communities in the Niger delta are 2 – 4 times the threshold level recommended by the Federal Environmental Protection

Agency (FEPA) and Department for Petroleum Resources (DPR). In a community in the region, the range of ambient concentration of SO_x is 92.0 – 430 µg/m^3 as against the 150 µg/m^3 recommended by the DPR.

Although, most of the flares in the region are vertical, there are some horizontal flares scattered around the neighbourhood of some communities. In horizontal flares, the downwind dispersal of emission is partially suppressed compared to vertical flares. This will cause an elevation of ambient level concentrations of air pollutants emanating from the flares.

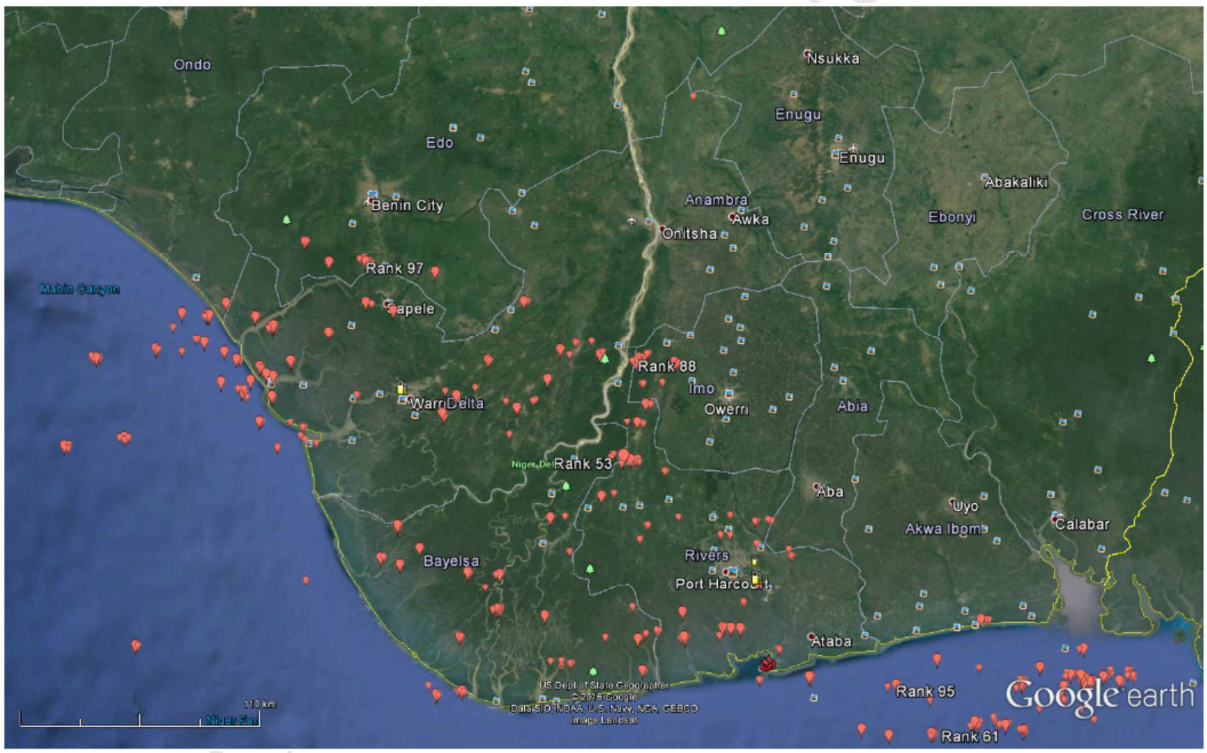

Figure 1: Google Earth imagery showing the Niger Delta. Red place-marks shows active flares (KML data for the flare locations are obtained from Elvidge et al. (2015))

3 Experimental design and methodology

This section gives a detailed explanation of the configuration of the model including the various combustion parameters and emission factors used in the simulation. An in-depth

description of the characteristics of the fuel and flares and meteorological variable implemented in the simulation is also carried out in this section.

The design and methodology adopted for this study is similar to that implemented in the study by Anejionu et al. (2015). While in their study, Anejionu et al. (2015), tried to assessed the contributions of the entire identified active flares in the region to air pollution in the country, this study tries to understand and assess the impact of monsoonal flow and flare characteristics on the dispersion pattern of emissions from real-world flares in the Niger Delta. It also suggested an effective mitigation process that could abate the seemingly intractable problem of bad air quality associated with gas flares in the study area.

3.1 Meteorological parameters

The prevailing wind in the region is the north-easterly monsoonal wind, but during the non-WAM months the south-westerly winds prevail. Due to the non-availability of adequate in-situ hourly meteorological data (wind speed, wind direction, cloud cover and relative humidity) in the study site, we have used Automated Surface Observing System (ASOS) data from a nearby airport in Cotonou, Benin, where sufficient hourly meteorological data needed for studies such as this is obtainable.

3.2 Combustion parameters estimates

Simulating the dispersion of emissions from high temperature sources such as gas flares requires adequate parameterization of the plume rise (Leahey and Davies, 1984; MoE Ontario, 2009; USEPA, 1995b). The following combustion parameters were computed using widely accepted methods available from the literature: (a) net heat released, H_r; (b) flame length, Δh; (c) buoyancy flux, F_b; (d) momentum flux, F_m; (e) effective diameter, D_{eff}.

$$H_r = \dot{m} \sum_{i=1}^{n} f_i H_i (1 - F_r) \quad \text{..... (1)} \qquad \text{(Beychok, 1994)}$$

$$\Delta h = 4.56 \times 10^{-3} \left(\frac{H_r}{4.1868}\right)^{0.478} \quad \text{..... (2)} \quad \text{(Beychok, 1994)}$$

Effective stack height = H + Δh ..... (3)

$$F_b = \frac{gH_r}{\pi C_p \rho_a T_a} \quad \text{..... (4)} \quad \text{(MoE Ontario, 2009)}$$

$$F_m = \frac{V_s H_r}{\pi C_p \rho_a (T_s - T_a)} \quad \text{..... (5)} \quad \text{(USEPA, 1995b)}$$

$$F_b = g V_s R_s{}^2 \left(\frac{T_s - T_a}{T_s}\right) \quad \text{..... (6)}$$

Equating the buoyancy flux from the flare (hot source) (Equation 4) to general buoyancy flux equation (Equation 6), while keeping other stack parameter constant yields the effective stack diameter:

$$D_{eff} = 0.1066 \sqrt{\frac{T_s}{T(T_s - T_a)} \times \frac{H_r}{V_s}} \quad \text{..... (7)}$$

where $\dot{m}$ - total molar flow rate to the flare

f_i - volume fraction of each hydrocarbon species in the fuel,

H_i - net heating value of each hydrocarbon species in the fuel (J/s),

H_r – net heat released by the fuel,

H – actual stack height,

F_r - fraction of radiative heat loss,

C_p – specific heat of dry air (J/kg.K),

T_a – ambient temperature (K),

g – acceleration due to gravity (m/s^2),

T_s – stack exit temperature (K),

V_s – exit velocity (m/s) , and

R_s – stack inner radius (m)

Although the fraction of heat loss depends on the combustion condition of the flare, we have, as recommended by the Alberta Environmental Agency (Alberta Environment, 2003), assumed a heat loss fraction of 25 %. The heat content of the fuel is calculated from the enthalpy of formation of its constituent alkane species and then reduced by 25 %. The net heat released by a typical gas flared in oil and gas fields across the globe varies significantly due to the large variation in the composition of natural gas from one field to another (Fawole et al., 2016a). Stack and fuel parameter used in the simulation is presented in Table S1.

3.3 Emission factors

In this study, we simulate the dispersion of particulate (black carbon, BC) and gaseous (carbon monoxide, CO) emissions from typical gas compositions and flare conditions in the Niger Delta area of Nigeria. We used emission factors of 1.6 gm^{-3} (Stohl et al., 2013) and 0.0067 kg/kg (EEMS, 2008) for black carbon (BC) and carbon monoxide (CO), respectively. The dispersion of other gaseous pollutants that are chemically passive on the timescale of plume dispersion (e.g., CO_2, SO_2, PAH) will scale linearly according to the ratio of their emission factors to that of CO.

$$\text{Emissions rate (g/s)} = A \times EF \times \left(1 - \frac{Eff}{100}\right) \quad \ldots\ldots\ldots\ldots\ldots\ldots\ldots\ldots\ldots\ldots \quad (8)$$ (USEPA, 1995a)

where: A – activity rate (in this case, the fuel volume flux (m^3/s))

EF – Emission factor (g/m^3)

Eff – emission reduction efficiency (%)

In this study, we have assumed flare efficiency to be 75 %, the upper limit of the 68±7 %, suggested by Leahey et al. (2001) in their study to assess the efficiencies of flares.

3.4 Experimental variables

The dispersion models (ADMS and AERMOD) are configured to assess the impact of the prevailing meteorology, fuel composition and flare capacity (in terms of volume flow flux) on the dispersion pattern and variation of ground-level concentrations of the flares considered in this study. While ADMS iteratively solves the plume rise calculations, AERMOD uses the Briggs formula to estimate the plume rise. Ground-level concentrations discussed in Section 4 are the mean monthly ground-level concentrations output from the models.

3.4.1 Prevailing meteorology during WAM and non-WAM months

The range of the wind speed is 3.0 – 5.7 ms^{-1} and 1.2 – 4.2 ms^{-1} during the WAM and non-WAM months, respectively. The relatively high mean wind speed during the WAM months is attributable to sea-breezes from the Gulf of Guinea. Figure 2 shows the wind roses of the non-WAM (DJF) and WAM (JJA) months considered in this study. The wind direction during the WAM month is predominantly North-easterly while in the non-WAM months, they are southerly, northerly and north-westerlies.

To assess the impact of prevailing meteorology on the dispersion of gas flaring emissions, we considered the dispersion pattern and ground-level concentrations of CO and BC, for real-world flares in the Niger Delta during the months of July and August; and December and January, which are the peaks of the WAM and non-WAM seasons.

3.4.2 Flare capacity (flow rate)

Two (one large and one small) flares in the study area were considered in this study. Globally, these flares are ranked 53rd and 363rd out of the over 7000 active flares identified by

Elvidge et al. (2015). For these two flares, the estimated total volumes of gas flared in 2012 are 0.278 and 0.0917 billion cubic meters (bcm) (Elvidge et al., 2015). With the assumption of a constant flow rate, the volume flow rates are 8.815 and 2.908 m^3s^{-1}, respectively. Volume flow rate influences the gas exit velocity and rate of heat released, and hence, the buoyancy and momentum of the plume exiting the flare.

3.4.3 Fuel composition

The composition of natural gas plays significant role in its thermodynamic properties. Although, assumed to be predominantly methane, the composition of natural gas varies significantly across oil fields (Fawole et al., 2016a). Using two very different fuels in terms of composition and density, the impact of fuel composition on the dispersion of emissions from gas flares is assessed. The emission factor of carbon monoxide (CO) used in this study is given as mass of pollutant per mass of natural gas ($kg.kg^{-1}$), and as such, the density of gas flared affects the CO emission rates. The composition, molar mass and density of the natural gas used are given in Table 1. These compositions are obtained from the literature.

Table 1: Fuel compositions used in this study (given in molar percentage)

	Less dense	**Denser**
CH_4	88.72	69.58
C_2H_6	5.93	0.25
C_3H_8	1.28	12.54
nC_4H_{10}	0.26	2.35
iC_4H_{10}	0.26	5.12
nC_5H_{12}	0.06	5.20
iC_5H_{12}	0.09	2.54
C_6H_{14}	0.06	1.97
C_7H_{16}	0.1	-
N_2	0.66	0.24
CO_2	2.55	0.21
H_2S	0.03	-
Molar mass	18.5	28.6

(g/mol)		
Density (kg/m^3)	0.75	1.2

267

268

269 **3.4.4 Plotting of spatial distribution of emissions**

270 The ADMS-ArcGIS link option in ArcMap 10.2 is employed to display ADMS outputs of

271 modelled pollutants as transparent filled contours on map of the region. An area of 80 by 85

272 km around the flare is used as the output grid in the model set-up.

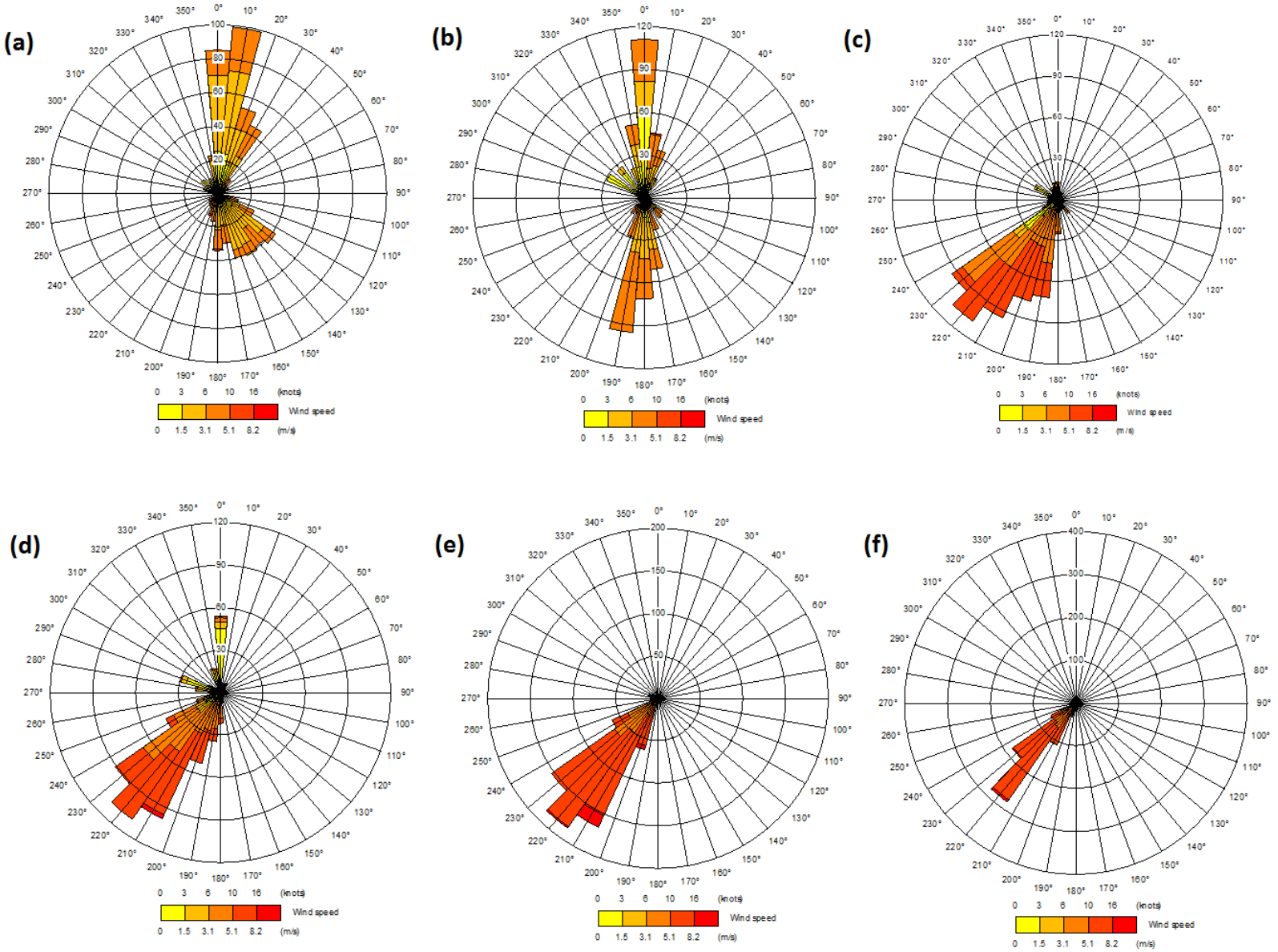

273

274 **Figure 2:** Wind roses (a) - (c) Non-WAM months – Dec., Jan. and Feb., respectively and (d) - (f) WAM months – Jun., Jul. and Aug., respectively.

4 Results and discussion

This section presents and discusses the simulated ground-level concentrations of CO and BC from the models as well as the impact of these concentrations of pollution level in the region. The influence of variables of interest on the concentration and dispersion of emissions from the flares is also examined and discussed.

4.1 Stack and natural gas parameters used in these simulations

The actual stack height, actual stack diameter, buoyancy flux, momentum flux, and effective height used for the two fuel compositions in these simulations are given in Table 2. Effective height, buoyancy flux and momentum flux are estimated using equations (3), (4) and (5), respectively.

Table 2: Stack and fuel parameters used

	Actual height (m)	**Actual diameter (m)**	**Buoyancy flux ($m^4.s^{-3}$)**	**Momentum flux ($m^4.s^{-2}$)**	**Effective height (m)**
Fuel I	20	0.75	638.7	137.7	42.8
Fuel II	20	0.75	1936.3	1265.5	49.4

4.2 Impact of prevailing meteorology

The impact of prevailing meteorology on the dispersion of emissions from gas flaring during the highly distinct seasons in the region is modelled for a two-year period (2014 and 2015). Ground-level concentrations and spatial distributions of the pollutant simulated are plotted on 80 by 85 km grid. The “smaller” flare, with a flow flux of 2.908 m^3s^{-1} and less-dense fuel composition was used to study the impact of meteorological variables on pollutant dispersion.

During the non-WAM months studied, that is, December and January, the dispersion of the emissions is in the direction of both the inland and coastal communities. The mean monthly ground-level concentration is greater towards the inland communities, probably due to the

higher speed of the north-easterly coastal wind compared to that of the south-westerly winds (see Figure 2). This pattern of dispersion is very similar for the four non-WAM months modelled. The 90^{th} and 95^{th} percentile of CO and BC mean monthly ground-level concentrations are in the range of 0.09 – 0.15 and 0.16 – 0.20 $\mu g.m^{-3}$ and; 0.02 – 0.03 and 0.03 – 0.04 $\mu g.m^{-3}$, respectively. The highest ranges of mean monthly ground-level concentration of CO and BC observed during these months are 0.73 - 1.81 $\mu g.m^{-3}$ and 0.15 - 0.36 $\mu g.m^{-3}$, respectively. As presented in the plots of spatial distribution in Figure 3, during the non-WAM months, emissions from this stack reaches more communities, albeit at a lower level of concentrations compared to the WAM months (see Figures 3 and 4), so there will be higher individual exposures during the WAM months, but greater population dose during the non-WAM months.

During the peak of the WAM months (July and August), the emissions are predominantly dispersed over the inland communities. As presented in the plots of the spatial distribution of ground-level concentration (Figure 4) and the percentiles below, spatial distribution of higher ground-level concentrations is greater during these months owing to the higher wind speeds in the WAM months compared to the non-WAM months (see section 3.4.1). The 90^{th} and 95^{th} percentile of CO and BC mean monthly ground-level concentrations are in the range of 0.02 – 0.11 and 0.2 – 0.25 $\mu g.m^{-3}$ and; 0.02 – 0.04 and 0.04 – 0.05 $\mu g.m^{-3}$, respectively. The highest range of monthly mean ground-level concentration of CO and BC during these months are in the ranges 0.62 - 0.99, and 0.12 - 0.2 $\mu g.m^{-3}$, respectively. Plots of spatial distribution of the pollutants from flares simulated as non-buoyant emission (a parametric extreme of flare simulation), during the WAM and non-WAM months considered are presented in the supplementary materials (see Figures S1 and S2).

It should be noted that this is just one of the over 300 active flares in the study area. Where dispersion plumes overlap, the combined ground-level concentration enhancement will be a

linear sum of the concentration from each overlapping plume. Results of these simulations show the level and pattern of dispersion during the peaks of the predominant seasons in the region. Considering the number and distribution of flares in the region and the spatial distribution of the level of pollutant ground-level concentration, the WAM months will be more severe period of poor air quality around the communities in the region. During the non-WAM months, there will be enhanced levels of BC, CO and other greenhouse gases (GHGs),

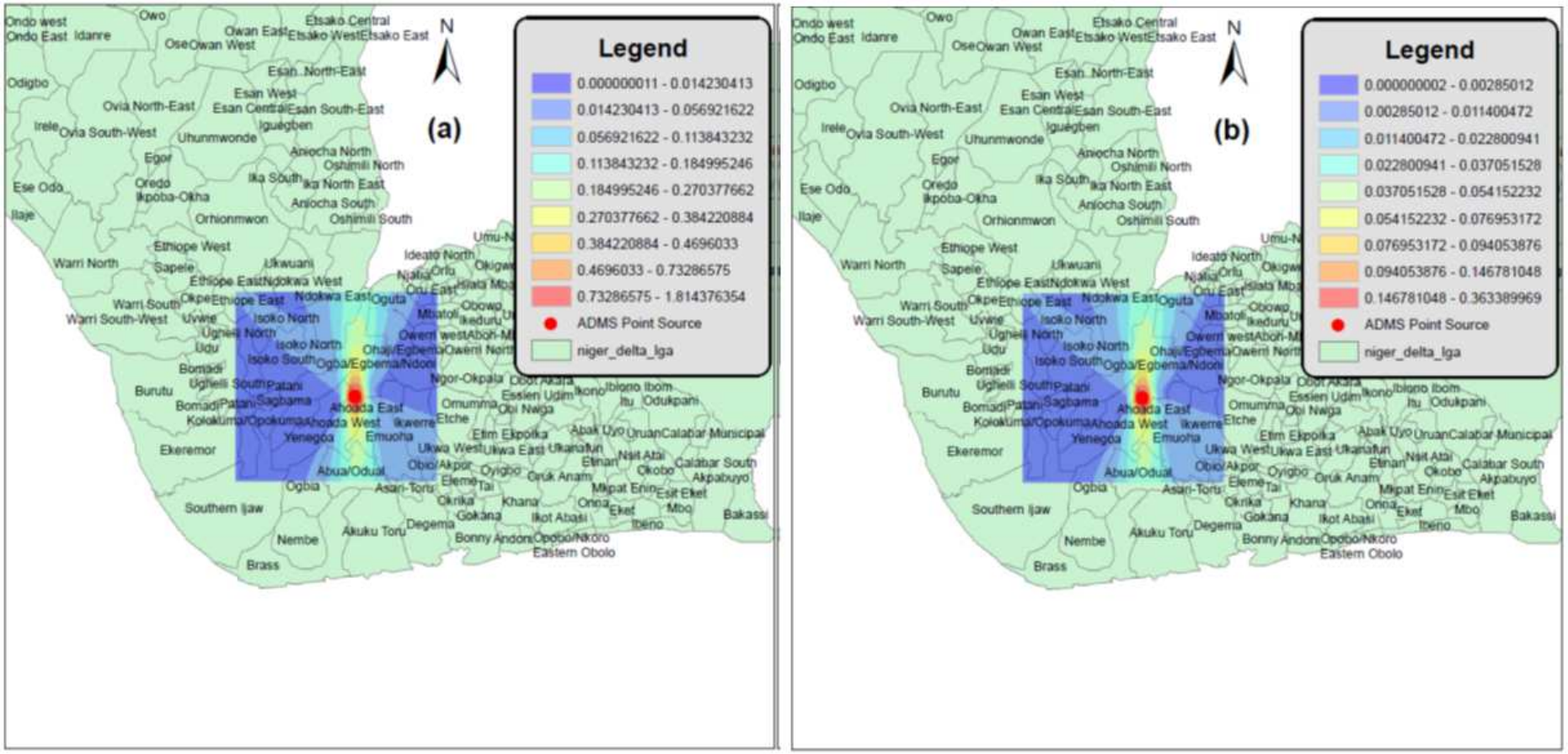

Figure 3: Modelled dispersion and mean monthly ground-level concentrations of (a) CO and (b) BC using fuel with lower heat content (fuel I) during a non-WAM month (Jan. 2015)

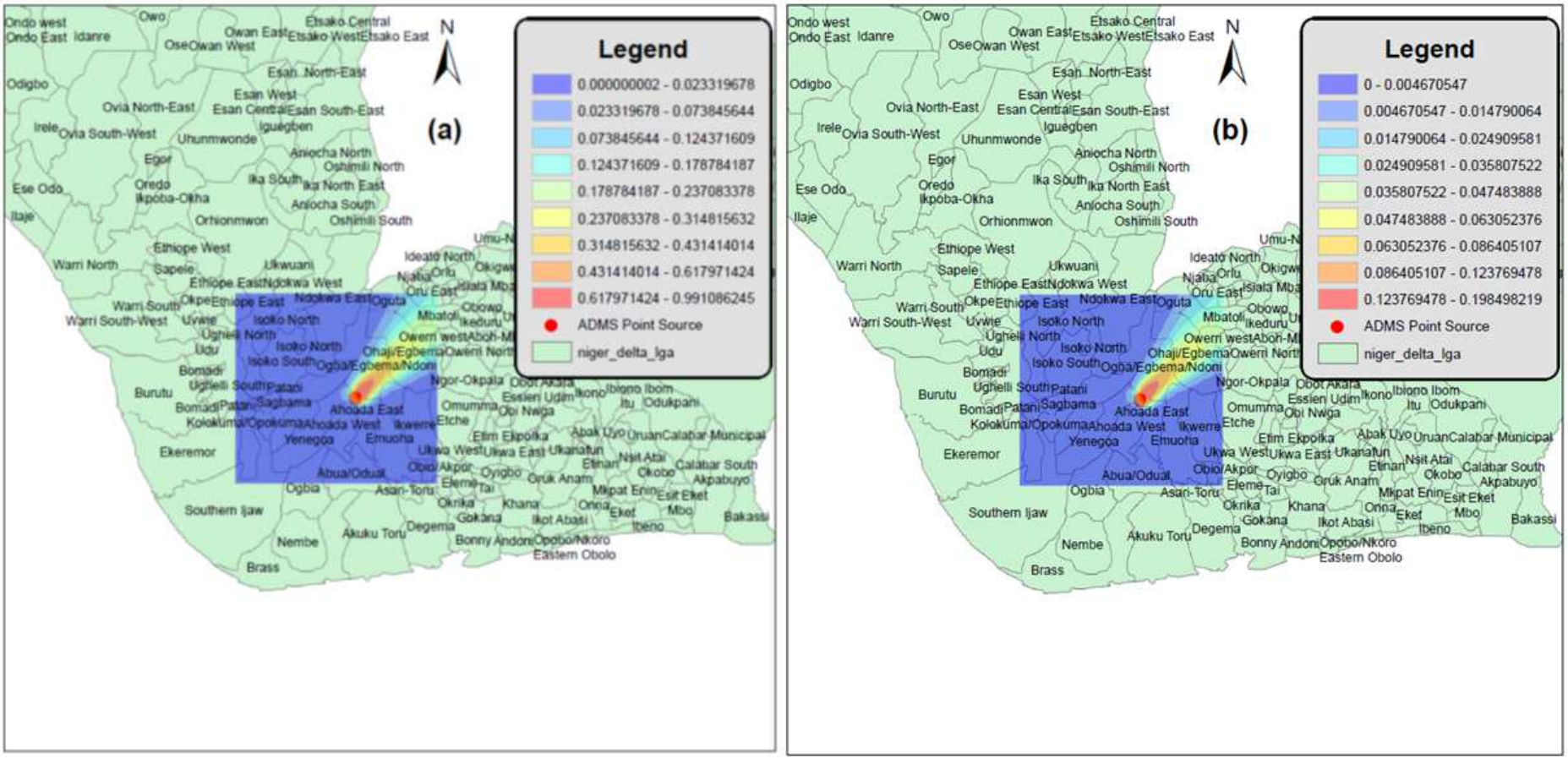

Figure 4: Modelled dispersion and mean monthly ground-level concentrations of (a) CO and (b) BC using fuel with lower heat content (fuel I) during a WAM months (Jul. 2015)

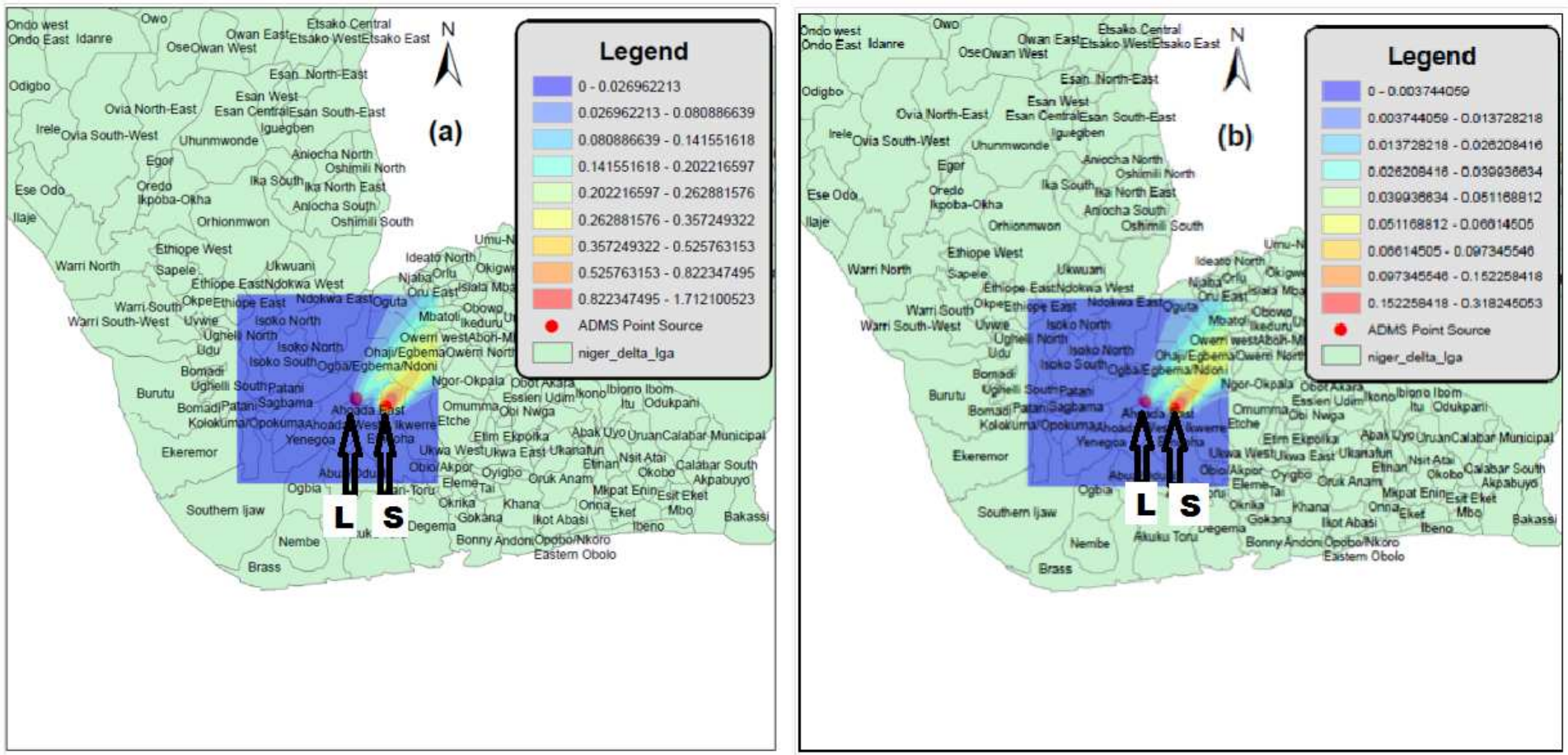

Figure 5: Modelled dispersion pattern and mean monthly ground-level concentration for (a) CO, and (b) BC from two flares of different sizes. "L" and "S" represent the large and small flare, respectively (Aug. 2014).

thereby significantly increasing aerosol optical depth (AOD) over the ocean around the Gulf of Guinea. The surface reflectance over the ocean is highly variant and is dependent on the atmospheric aerosol loading (Jin et al., 2004). Hence, the Earth-atmosphere radiative budget in the region over the ocean might be significantly perturbed during this period.

Modelling flares as a non-buoyant source gives significant difference to the monthly mean ground-level concentrations. For example, for a typical non-WAM month (Jan. 2015), the highest range of monthly mean ground-level concentration of CO and BC are 8.65 - 13.96 $\mu g.m^{-3}$ and 1.73 - 2.79 $\mu g.m^{-3}$, respectively. Plots of spatial distribution of pollutants in flare modelled as non-buoyant sources are given in the supplementary material.

4.3 Impact of flare capacity

Flare capacity, that is, the volume flow rate of the fuel (m^3s^{-1}) in the stack, is a determinant of the emission rate (gs^{-1}) of pollutants used in modelling the dispersion of pollutants from a source. The volume flow rate contributes to the magnitude of the buoyancy and momentum flux of the plume as it determines the exit velocity of the fuel into the flame as well as the heat release rates.

Using the two real-world flares discussed in section 3.4.2, the dispersion of CO and BC from flares of different sizes under the same atmospheric condition was modelled. In Figure 5, "L" and "S" represent the large and small flare, respectively. The higher concentration in the tail of the dispersion pattern for the “small” flare (see Figure 5) is as a result of the lower buoyancy of the plume exiting the stack. The lower buoyancy is occasioned by the lower exit velocity of the fuel into the flame. The region of higher concentration is further downwind in the large flare (see Figure 5). The highest ground-level concentration of the two flares differs by a factor of about 4.

Instead of flaring gas from stacks at flow stations with low volume flux, two or more of such flares could be linked up to enhance the volume flow rate and increasing the stack height, so as to reduce the ground-level concentrations of pollutants.

4.4 Impact of fuel composition

The composition of natural gas flared affects the ground-level concentration and dispersion pattern of emissions from real-world flares. It affects the quantity of radiant heat given off, effective height and effective diameter, all of which are essential determinants in the dispersion of emission from the flare. The thermodynamic parameters calculated from the two compositions of natural gas considered in this study are presented in Table 2. The plume exiting the stack for the fuel with less heat content (less dense fuel) is less buoyant, and hence the ground-level concentrations are higher and the distance downwind at which this higher ground-level concentration is observed, is shorter than that for the fuel with the higher heat content (dense fuel).

Meteorological data for August 2015 is used to study and assess the impact of fuel composition on the dispersion pattern and ground-level concentration of pollutants from real-world flares in the study area. For the less dense fuel, the 90^{th} and 95^{th} percentile of CO and BC ground-level concentrations are 0.11 and 0.21 $\mu g.m^{-3}$, and 0.02 and 0.04 $\mu g.m^{-3}$, respectively. The range of the highest ground-level concentration of CO and BC are 0.62 - 0.92 and 0.13 - 0.19 $\mu g.m^{-3}$, respectively. For the dense fuel, the 90^{th} and 95^{th} percentile of CO and BC ground-level concentrations are 0.05 and 0.1 $\mu g.m^{-3}$, and 0.01 and 0.02 $\mu g.m^{-3}$, respectively, while the range of the highest ground-level concentration of CO and BC are 0.14 - 0.17 and 0.03 - 0.04 $\mu g.m^{-3}$, respectively.

Although, the range of highest ground-level concentrations of CO and BC for the two fuel compositions during periods considered in this study varies substantially, their 90^{th} and 95^{th}

385 percentiles of CO and BC ground-level concentrations vary by a factor of about 2. A fact,
386 once again, underpinning the importance of adequate knowledge of the composition of the
387 gas flared in order to be able to quantify its contribution to ambient aerosol loading.

388 The emission factor for CO used in this study, as stated in section 3.3, is dependent on the
389 density of the fuel. Hence, the emission factor used for the less dense and denser fuel
390 compositions is 11.02 and 17.63 $g.m^{-3}$, respectively. Figure 6 and 7 shows the plots of the
391 spatial distribution of ground-level concentration of pollutants emitted from the flare for the
392 denser and less dense fuel compositions, respectively. From Figure 7, the ground-level
393 concentration within the proximity of the flare is higher than that for the denser fuel
394 composition in Figure 6.

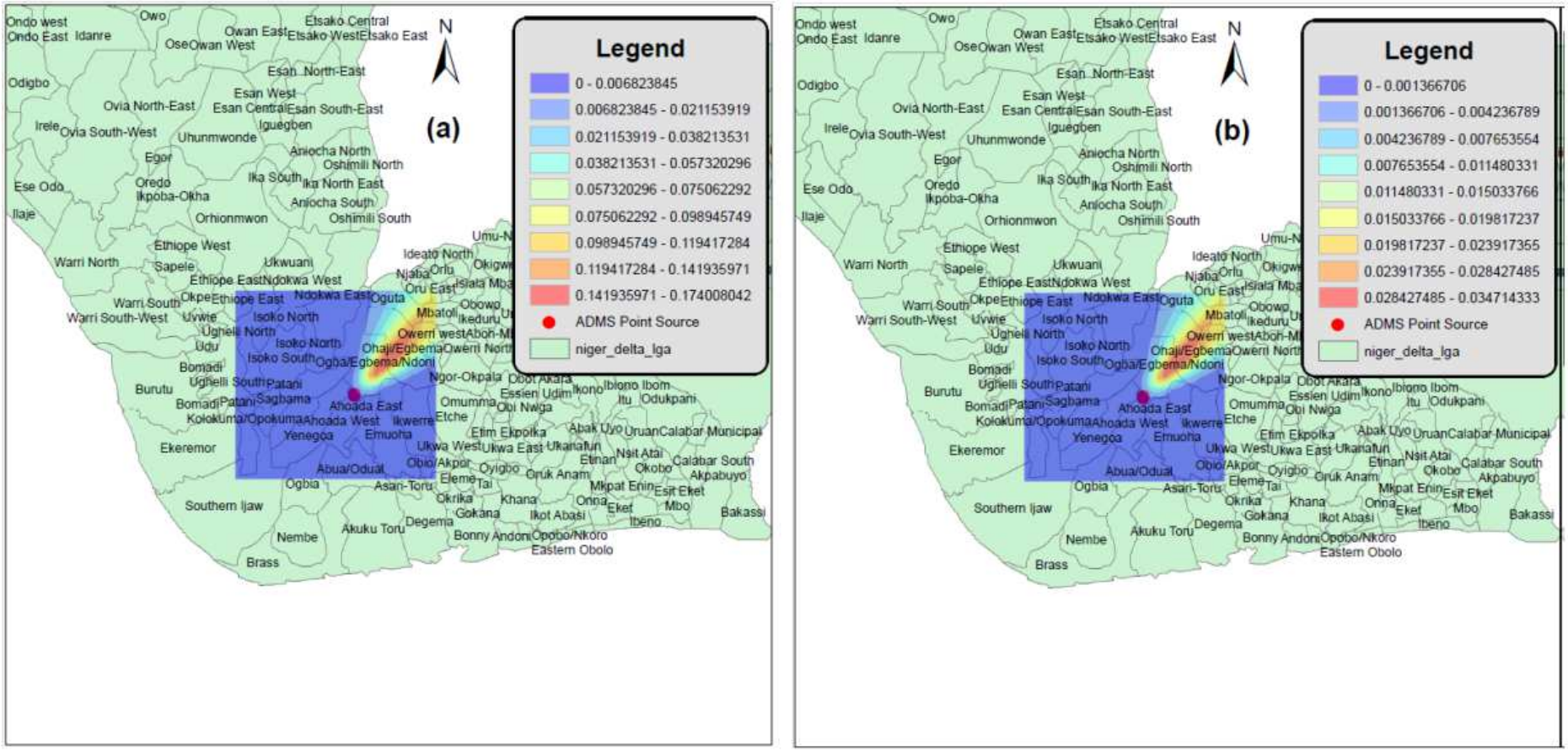

Figure 6: Dispersion pattern and mean monthly ground-level concentration of (a) CO and (b) BC for the denser fuel composition (Aug. 2015).

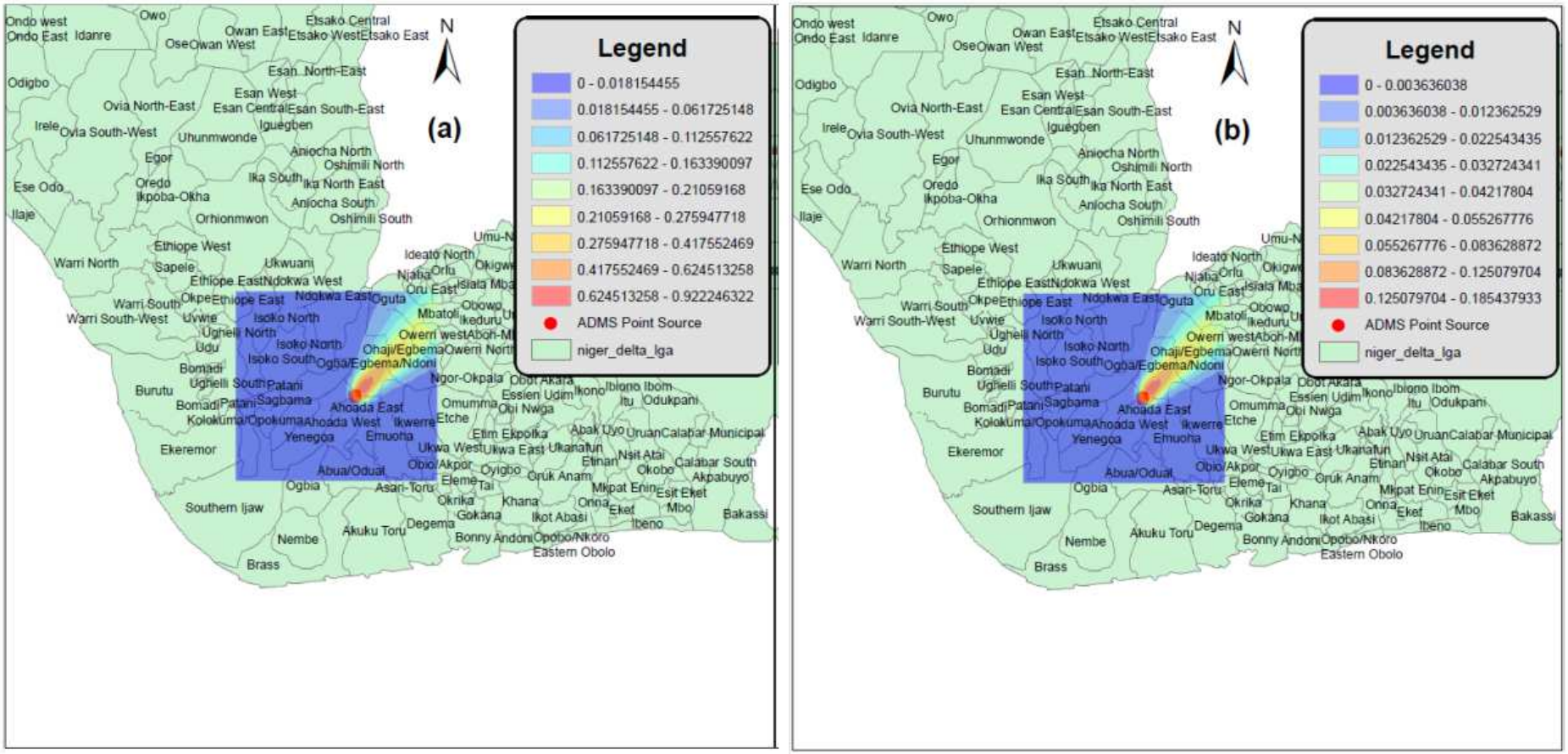

Figure 7: Dispersion pattern and mean monthly ground-level concentration of (a) CO and (b) BC for for the less dense fuel composition (Aug. 2015).

4.5 AERMOD simulations

AERMOD estimates of BC and CO dispersions in WAM (August) and non-WAM (January) months of 2015 (Figure 8) were compared with UK-ADMS projections for small-flare low-density fuel source characteristics. The 90^{th} and 95^{th} percentile of mean monthly ground-level concentrations of BC and CO for non-WAM month are 0.06 and 0.09, and 0.18 and 0.29, respectively. For the WAM month, the values are 0.05 and 0.10; and 0.17 and 0.32, respectively. Although, the predominant ventilation corridors resulting from the AERMOD simulation is largely the same with ADMS, its concentrations are higher by a factor of 1.5 for CO and 2.5 for BC in the WAM months. The variances in estimates from the two models can be linked to differences in their formulations. In AERMOD, if the boundary layer is stable, only two limits for the horizontal dispersion are considered: the coherent plume limit generated by shifting wind and the random plume limit when the plume spread is assumed uniformly distributed throughout the area (Cimorelli et al., 2005; Perry et al., 2005; Venkatram et al., 2004). It should also be noted that surface albedo inputs in this case were taken from literature values (Jegede et al., 1997). Nevertheless, AERMOD values were much lower compared with the non-buoyant source estimates from ADMS taking January 2015 as a typical scenario. This clearly indicates that AERMOD estimates for pollutants dispersion from the gas flares are within acceptable limits of parametric extremes of ADMS (i.e. buoyant and non-buoyant source estimates).

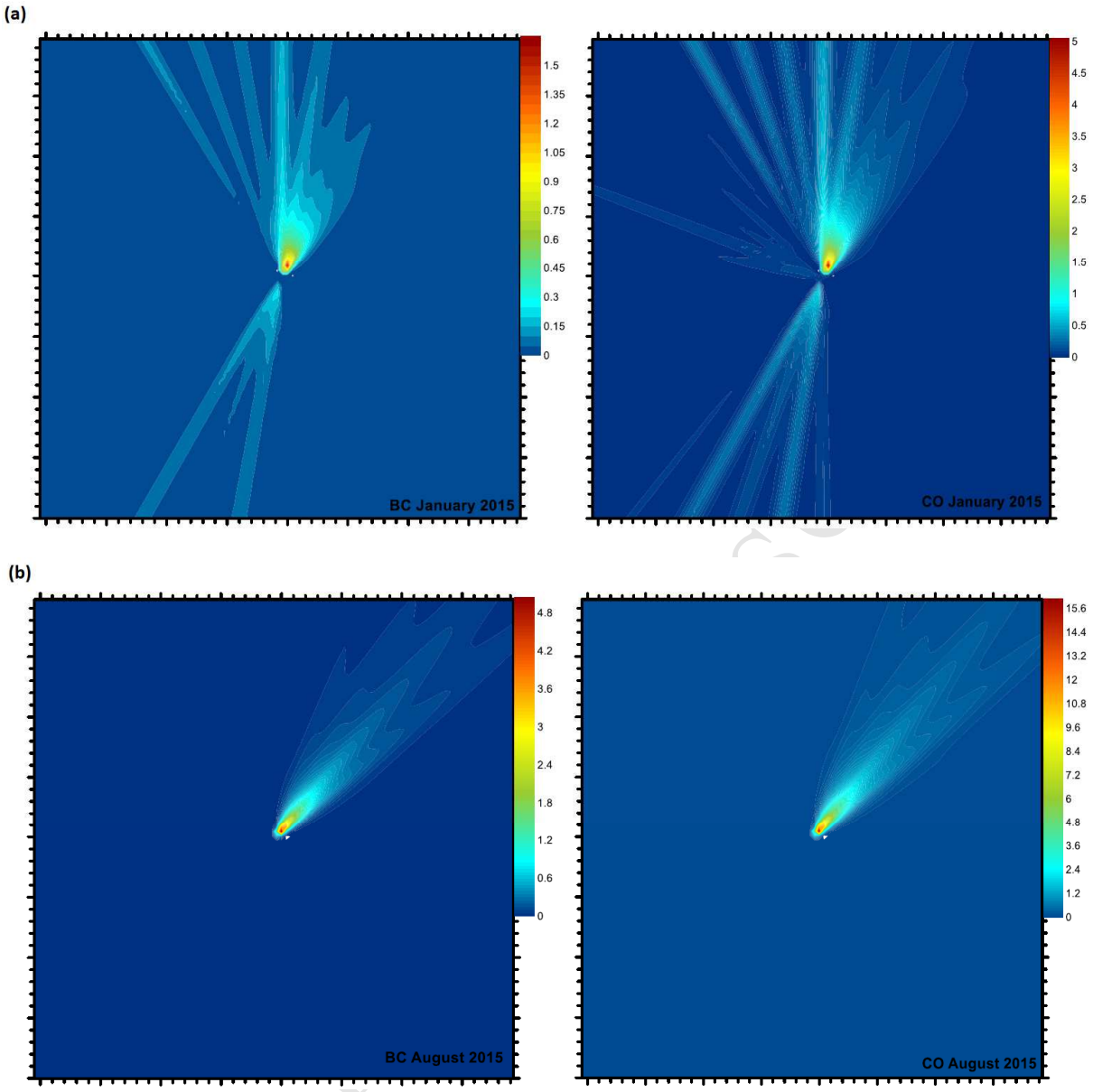

Figure 8: : Modelled (AERMOD) dispersion and monthly mean ground-level concentrations of BC and CO for (a) non-WAM (Jan 2015) and (b) WAM (August 2015) using fuel with lower heat content (fuel I).

5 Conclusions

This work assesses the impact of fuel composition, flare size and meteorological parameter on the dispersion and ground-level concentrations of carbon monoxide and black carbon. Although the actual height and diameter of the real-world flares used in this study are not known, we have tried to use values obtained for similar flares in the literature. During the non-WAM months, emissions are dispersed both towards the communities inland and on the

coast, though with lesser concentration level compared to the WAM months. Hence, higher individual exposures are experienced during the WAM months, but greater population dose during the non-WAM months. The ground-level concentration around the inland communities is higher in the WAM months. The significant impact of prevailing meteorology on ground-level concentrations and dispersion pattern of emissions from active flares is also corroborated by simulations carried out with AERMOD.

Rather than use shorter stacks to flare gas at flow stations with low volume flow flux, and hence, strongly enhancing ground-level concentration of pollutant, it is suggested that two or more of such stations be linked together to increase the volume flow flux. Increasing volume flow flux increases the buoyancy and momentum flux of the plume emanating from such stacks, and thereby, reducing ground-level concentrations.

6 Acknowledgement

Olusegun G. Fawole is highly grateful to the UK government for funding his PhD studies through the UK Commonwealth Scholarships Commission (CSCUK) NGCA-2013-70.

456

457 7 References

458 Abiye, O., Sunmonu, L., Ajao, A., Akinola, O., Ayoola, M. and Jegede, O., 2016.
459 Atmospheric dispersion modeling of uncontrolled gaseous pollutants (SO2 and NOX)
460 emission from a scrap-iron recycling factory in Ile-Ife, Southwest Nigeria. Cogent
461 Environmental Science, 2(1): 1275413.
462 Adoki, A., 2012. Air quality survey of some locations in the Niger Delta Area. Journal of
463 Applied Sciences and Environmental Management, 16(1): 125-134.
464 Adole, T., 2011. A GIS based assessment of the impact of gas flaring on vegetation cover in
465 Delta state, Nigeria, University of East Anglia, United Kingdom, 107 pp.
466 Alberta Environment, 2003. Emergency/Process Upset Flaring Management: Modelling
467 Guidance, Science and Standards Branch, Alberta Environment, Edmonton, Alberta.
468 Ana, G., Sridhar, M. and Emerole, G., 2012. Polycyclic aromatic hydrocarbon burden in
469 ambient air in selected Niger Delta communities in Nigeria. Journal of the Air & Waste
470 Management Association, 62(1): 18-25.
471 Anejionu, O.C., Whyatt, J.D., Blackburn, G.A. and Price, C.S., 2015. Contributions of gas
472 flaring to a global air pollution hotspot: Spatial and temporal variations, impacts and
473 alleviation. Atmospheric Environment, 118: 184-193.
474 Anomohanran, O., 2012. Determination of greenhouse gas emission resulting from gas
475 flaring activities in Nigeria. Energy Policy, 45: 666-670.
476 Arya, S.P., 1999. Air pollution meteorology and dispersion. Oxford University Press (OUP),
477 New York.
478 Beychok, M.R., 1994. Fundamentals of stack gas dispersion, 63. Milton R. Beychok Irvine.
479 Carruthers, D., Edmunds, H., Bennett, M., Woods, P., Milton, M., Robinson, R., Underwood,
480 B., Franklin, C. and Timmis, R., 1997. Validation of the ADMS dispersion model and
481 assessment of its performance relative to R–91 and ISC using archived LIDAR data.
482 International Journal of Environment and Pollution, 8(3-6): 264-278.
483 Cimorelli, A.J., Perry, S.G., Venkatram, A., Weil, J.C., Paine, R.J., Wilson, R.B., Lee, R.F.,
484 Peters, W.D. and Brode, R.W., 2005. AERMOD: A dispersion model for industrial
485 source applications. Part I: General model formulation and boundary layer
486 characterization. Journal of applied meteorology, 44(5): 682-693.

Connan, O., Leroy, C., Derkx, F., Maro, D., Hébert, D., Roupsard, P. and Rozet, M., 2011. Atmospheric dispersion of an elevated release in a rural environment: Comparison between field SF 6 tracer measurements and computations of Briggs and ADMS models. Atmospheric environment, 45(39): 7174-7183.

Dung, E.J., Bombom, L.S. and Agusomu, T.D., 2008. The effects of gas flaring on crops in the Niger Delta, Nigeria. GeoJournal, 73(4): 297-305.

Ede, P.N. and Edokpa, D.O., 2015. Regional air quality of the Nigeria's Niger delta. Open Journal of Air Pollution, 4(1): 7-15.

EEMS, 2008. Atmospheric emissions calculations, Environmental Emissions Monitoring System, United Kingdom.

Elvidge, C.D., Zhizhin, M., Baugh, K., Hsu, F.-C. and Ghosh, T., 2015. Methods for Global Survey of Natural Gas Flaring from Visible Infrared Imaging Radiometer Suite Data. Energies, 9(1): 14.

Elvidge, C.D., Ziskin, D., Baugh, K.E., Tuttle, B.T., Ghosh, T., Pack, D.W., Erwin, E.H. and Zhizhin, M., 2009. A fifteen year record of global natural gas flaring derived from satellite data. Energies, 2(3): 595-622.

Fawole, O., Cai, X.-M. and MacKenzie, A., 2016a. Gas flaring and resultant air pollution: A review focusing on Black Carbon. Environmental Pollution, 216: 182-197. doi: 10.1016/j.envpol.2016.05.075.

Fawole, O.G., Cai, X., Levine, J.G., Pinker, R.T. and MacKenzie, A., 2016b. Detection of a gas flaring signature in the AERONET optical properties of aerosols at a tropical station in West Africa. Journal of Geophysical Research: Atmospheres, 121(24): 14513–14524.

Fawole, O.G., Cai, X. and MacKenzie, A., 2017. Evidence for a gas-flaring source of alkanes leading to elevated ozone in air above West Africa. African Journal of Environmental Science and Technology, 11(10): 532-543.

Gryparis, A., Forsberg, B., Katsouyanni, K., Analitis, A., Touloumi, G., Schwartz, J., Samoli, E., Medina, S., Anderson, H.R. and Niciu, E.M., 2004. Acute effects of ozone on mortality from the "air pollution and health: a European approach" project. American journal of respiratory and critical care medicine, 170(10): 1080-1087.

Heist, D., Isakov, V., Perry, S., Snyder, M., Venkatram, A., Hood, C., Stocker, J., Carruthers, D., Arunachalam, S. and Owen, R.C., 2013. Estimating near-road pollutant dispersion: A model inter-comparison. Transportation Research Part D: Transport and Environment, 25: 93-105.

IPCC (Editor), 2013. Summary for Policymakers. In: Climate Change 2013: The Physical Science Basis. Contribution of Working Group I to the Fifth Assessment Report of the Intergovernmental Panel on Climate Change. Cambridge University Press, Cambridge, United Kingdom and New York, USA.

Ite, A.E. and Ibok, U.J., 2013. Gas Flaring and Venting Associated with Petroleum Exploration and Production in the Nigeria's Niger Delta. American Journal of Environmental Protection, 1(4): 70-77.

Jegede, O., Fasheun, T., Adeyefa, Z. and Balogun, A., 1997. The effect of atmospheric stability on the surface-layer characteristics in a low-wind area of tropical West Africa. Boundary-Layer Meteorology, 85(2): 309-323.

Jin, Z., Charlock, T.P., Smith, W.L. and Rutledge, K., 2004. A parameterization of ocean surface albedo. Geophysical research letters, 31(22).

Johnson, M., Devillers, R. and Thomson, K., 2013. A Generalized Sky-LOSA Method to Quantify Soot/Black Carbon Emission Rates in Atmospheric Plumes of Gas Flares. Aerosol Science and Technology, 47(9): 1017-1029.

Kampa, M. and Castanas, E., 2008. Human health effects of air pollution. Environmental pollution, 151(2): 362-367.

Leahey, D. and Davies, M., 1984. Observations of plume rise from sour gas flares. Atmospheric Environment (1967), 18(5): 917-922.

Leahey, D.M., Preston, K. and Strosher, M., 2001. Theoretical and observational assessments of flare efficiencies. Journal of the Air & Waste Management Association, 51(12): 1610-1616.

Marais, E.A., Jacob, D., Wecht, K., Lerot, C., Zhang, L., Yu, K., Kurosu, T., Chance, K. and Sauvage, B., 2014. Anthropogenic emissions in Nigeria and implications for atmospheric ozone pollution: A view from space. Atmospheric Environment, 99: 32-40.

MoE Ontario, 2009. Air dispersion modelling guideline for Ontario (Version 2.0), Ontario Minstry of Environment, Ontario, Canada (https://www.ontario.ca/document/guideline-11-air-dispersion-modelling-guideline-ontario).

OPEC, 2015. OPEC annual statistical bulletin, Organisation of Petroleum Exporting Countries, Austria.

Osuji, L.C. and Onojake, C.M., 2004. Trace Heavy Metals Associated with Crude Oil: A Case Study of Ebocha-8 Oil-Spill-Polluted Site in Niger Delta, Nigeria. Chemistry & biodiversity, 1(11): 1708-1715.

553 Perry, S.G., Cimorelli, A.J., Paine, R.J., Brode, R.W., Weil, J.C., Venkatram, A., Wilson,
554 R.B., Lee, R.F. and Peters, W.D., 2005. AERMOD: A dispersion model for industrial
555 source applications. Part II: Model performance against 17 field study databases. Journal
556 of applied meteorology, 44(5): 694-708.
557 Pope III, C., 2000. Epidemiology of fine particulate air pollution and human health: biologic
558 mechanisms and who's at risk? Environmental health perspectives, 108(Suppl 4): 713.
559 Pope III, C.A., Burnett, R.T., Thun, M.J., Calle, E.E., Krewski, D., Ito, K. and Thurston,
560 G.D., 2002. Lung cancer, cardiopulmonary mortality, and long-term exposure to fine
561 particulate air pollution. Journal of American Medical Association, 287(9): 1132-1141.
562 Pope III, C.A. and Dockery, D.W., 2006. Health effects of fine particulate air pollution: lines
563 that connect. Journal of the Air & Waste Management Association, 56(6): 709-742.
564 Stohl, A., Klimont, Z., Eckhardt, S., Kupiainen, K., Shevchenko, V., Kopeikin, V. and
565 Novigatsky, A., 2013. Black carbon in the Arctic: the underestimated role of gas flaring
566 and residential combustion emissions. Atmospheric Chemistry and Physics, 13(17):
567 8833-8855.
568 Sultan, B. and Janicot, S., 2000. Abrupt shift of the ITCZ over West Africa and intra-seasonal
569 variability. Geophysical Research Letters, 27(20): 3353-3356.
570 Sultan, B. and Janicot, S., 2003. The West African monsoon dynamics. Part II: The
571 “preonset” and “onset” of the summer monsoon. Journal of climate, 16(21): 3407-3427.
572 Turner, D.B., 1994. Workbook of atmospheric dispersion estimates: an introduction to
573 dispersion modeling. CRC press.
574 USEPA, 1995a. AP 42-Compilation of air pollutant emission factors. Section 13.5: Industrial
575 flares, U.S Environmental Protection Agenecy, Office of Air quality planning and
576 standards, Research Triangle Park, NC.
577 http://www.epa.gov/ttn/chief/ap42/ch13/final/c13s05.pdf.
578 USEPA, 1995b. SCREEN3 Model User’s Guide. EPA-454/B-95-004 U.S. Environmental
579 Protection Agency, Research Triangle Park, NC, USA.
580 USEPA, 2011. Emission Estimation Protocol for Petroleum Refineries, US Environmental
581 Protection Agency, Washington, DC.
582 USEPA, 2012. Report to congress on Black Carbon. EPA-450/R-12-001, United States
583 Environmental Protection Agency, Research Triangle Park, NC.
584 Venkatram, A., Isakov, V., Yuan, J. and Pankratz, D., 2004. Modeling dispersion at distances
585 of meters from urban sources. Atmospheric Environment, 38(28): 4633-4641.
586 Young, E.M., 2013. Food and development. Routledge, Oxon, United Kingdom.

587 Zannetti, P., 2013. Air pollution modeling: theories, computational methods and available
588 software. Springer Science & Business Media.

589

Highlights

- During monsoonal flow ambient ground-level concentrations are higher and inland.
- There is higher individual exposure during the WAM (West African Monsoon) months.
- There is greater population dose during the non-WAM months.
- Flare and fuel characteristics play major roles in emissions yields from flares.
- Both ADMS and AERMOD are adequate for simulating emissions from gas flares.